

## Friction Between a Viscoelastic Body and a Rigid Surface with Random Self-Affine Roughness

Q. Li,<sup>1</sup> M. Popov,<sup>1</sup> A. Dimaki,<sup>2</sup> A. E. Filippov,<sup>3</sup> S. Kürschner,<sup>1</sup> and V. L. Popov<sup>1,\*</sup>

<sup>1</sup>*Berlin University of Technology, 10623 Berlin, Germany*

<sup>2</sup>*Institute of Strength Physics and Materials Science, Russian Academy of Sciences, 634021 Tomsk, Russia*

<sup>3</sup>*Donetsk Institute for Physics and Engineering of NASU, 83114 Donetsk, Ukraine*

(Received 13 May 2013; revised manuscript received 13 June 2013; published 17 July 2013)

In this Letter, we study the friction between a one-dimensional elastomer and a one-dimensional rigid body having a randomly rough surface. The elastomer is modeled as a simple Kelvin body and the surface as self-affine fractal having a Hurst exponent  $H$  in the range from 0 to 1. The resulting frictional force as a function of velocity always shows a typical structure: it first increases linearly, achieves a plateau and finally drops to another constant level. The coefficient of friction on the plateau depends only weakly on the normal force. At lower velocities, the coefficient of friction depends on two dimensionless combinations of normal force, sliding velocity, shear modulus, viscosity, rms roughness, rms surface gradient, the linear size of the system, and the Hurst exponent. We discuss the physical nature of different regions of the law of friction and suggest an analytical relation describing the coefficient of friction in a wide range of loading conditions. An important implication of the analytical result is the extension of the well-known “master curve procedure” to the dependencies on the normal force and the size of the system.

DOI: [10.1103/PhysRevLett.111.034301](https://doi.org/10.1103/PhysRevLett.111.034301)

PACS numbers: 46.55.+d, 62.20.Qp, 81.40.Pq

Since classical works by Bowden and Tabor [1], it is widely accepted that the roughness plays a central role in friction processes. Greenwood and Tabor [2] have shown that the friction of elastomers can be attributed to deformation losses in the elastomer. In 1963, Grosch supported this idea by a series of experiments of friction between rubber and hard surfaces with controlled roughness [3]. In the following years, the basic understanding of the role of rheology [4] and of surface roughness [5,6] in elastomer friction has been achieved. Most works on elastomer friction discuss the coefficient of friction, thus implicitly implying the validity of Amontons’ law: the force of friction is proportional to the normal load; the coefficient of friction is considered to be a quantity which does not depend on the normal load [7,8]. However, it is well known that this law is only a very rough first approximation and that both the static and the sliding coefficient of friction, even between the same material pairing, can change by a factor of about 4 depending on the geometry of a tribological system as a whole and loading conditions. The load dependence of the elastomer friction was studied experimentally by Schallamach [9]. In a more general context, the strong violations of Amontons’ law were studied experimentally and theoretically in recent papers [10,11]. Deviations from Amontons’ law can be due to macroscopic interfacial dynamics [12–14] or they can be connected with the contact mechanics of rough surfaces. This Letter is devoted to a study of elastomer friction beyond the regions of validity of Amontons’ law due to purely contact mechanical reasons. To achieve the basic understanding of this nonlinear frictional behavior, we consider the following simple model: (i) the elastomer is modeled as a simple Kelvin body, which is completely characterized by its

static shear modulus and viscosity, (ii) the nondisturbed surface of the elastomer is plane and frictionless, (iii) the rigid counter body is assumed to have a randomly rough, self-affine fractal surface without long wave cutoff, (iv) no adhesion or capillarity effects are taken into account, and (v) we consider a one-dimensional model. These simple assumptions still result in nontrivial and complicated frictional behavior.

We do not claim that the reported results can be directly applied for the friction of a true three-dimensional elastomer. However, we would like to note that there is evidence coming from recent studies of contact mechanics of both rotationally symmetric profiles [15,16] and self-affine fractal surfaces [17,18] that suggest that the results obtained with one-dimensional foundations may have a broad area of applicability if the rules of the method of dimensionality reduction (MDR) [19–21] are applied. Following this method, the elastomer was modeled as a row of independent elements with a small spacing  $\Delta x$ , each element consisting of a spring with normal stiffness  $\Delta k = 4G\Delta x$  and a dashpot having the damping constant  $\Delta d = 4\eta\Delta x$ , where  $G$  is the shear modulus and  $\eta$  the viscosity of the elastomer. The counter body was a rough line having the power spectral density  $C_{1D} \propto q^{-2H-1}$ , where  $q$  is the wave vector and  $H$ , the Hurst exponent. The spectral density was defined in the interval from  $q_{\min} = 2\pi/L$ , where  $L$  is the system size, to the upper cutoff wave vector  $q_{\max} = \pi/\Delta x$ . The spacing  $\Delta x$  determines the upper cutoff wave vector and is an essential physical parameter of the model. Surface topography was characterized by the rms roughness  $h = [2 \int_{q_{\min}}^{q_{\max}} C_{1D}(q) dq]^{1/2}$ , which is dominated by the long wavelength components of the power spectrum and the rms gradient of the surface  $\nabla z = [2 \int_{q_{\min}}^{q_{\max}} C_{1D}(q) q^2 dq]^{1/2}$ ,

dominated by the short wavelength part of the spectrum. The rigid surface was generated according to the rules described in [21], and periodic boundary conditions were used. The rigid surface was pressed against the elastomer with a normal force  $F_N$  and moved tangentially with a constant velocity  $v$ .

If the rigid profile is given by  $z = z(x - vt)$ , and the profile of the elastomer by  $u = u(x, t)$ , then the normal force in each particular element of the viscoelastic foundation is given by

$$f = -4\Delta x\{Gu(x) + \eta\dot{u}(x, t)\}. \quad (1)$$

For the elements in contact with the rigid surface, this means that

$$f = 4\Delta x\{G[d - z(x, t)] + \eta v z'(x, t)\}, \quad (2)$$

where  $d$  is the indentation depth. For these elements, the condition of remaining in contact,  $f > 0$ , was checked in each time step. Elements out of contact were relaxed according to equation  $f = 0$ :  $Gu(x) + \eta\dot{u}(x, t) = 0$ , and the noncontact condition  $u < z$  was checked. The indentation depth  $d$  was determined to satisfy the condition of the constant normal force

$$F_N = 4 \int_{(\text{real cont})} [G(d - z(x)) + \eta v z'(x)] dx, \quad (3)$$

where the integration is only over points in contact. A typical configuration of the contact is shown in Fig. 1. The tangential force was calculated by multiplying the local normal force in each single element with the local surface gradient and subsequently summing over all elements in contact

$$F_x = -4 \int_{(\text{real cont})} z'(x)[G(d - z(x)) + \eta v z'(x)] dx. \quad (4)$$

Because of the independence of the degrees of freedom, the algorithm is not iterative and there are no convergence problems.

The one-dimensional model is computationally efficient and allows carrying out extensive parameter studies. The following ranges of parameters have been covered in the present study. The length of the system was  $L = 0.02$  m and the number of elements  $N = L/\Delta x$  was typically 5000 with exception of cases where the dependence on  $\Delta x$  was studied. Instead of viscosity, the relaxation time  $\tau = \eta/G = 10^{-3}$  s was used. 11 values of Hurst exponent ranging from 0 to 1 were studied. All values shown below were obtained by averaging over 200 realizations of the rough surface for each set of parameters. Parameter studies have been carried out for 20 different normal forces  $F_N$ , ranging from  $10^{-3}$  to  $10^2$  N, 20 values of the  $G$  modulus from  $10^3$  to  $10^9$  Pa, 20 values of rms roughness  $h$  from  $10^{-9}$  to  $10^{-5}$  m, and 20 values of the spacing  $\Delta x$  from  $10^{-5}$  to  $10^{-7}$  m, while in each simulation series only one parameter was varied. The presented results are based on approximately  $3.5 \times 10^6$  single simulations with the total net computation time of about 50 h. It is well known that the maximum value of the

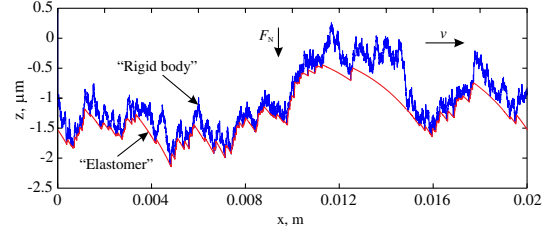


FIG. 1 (color online). One-dimensional contact between a rough surface and a viscoelastic elastomer. Note the difference in vertical and horizontal units.

coefficient of friction  $\mu$  in the medium range of velocities is proportional to the rms gradient of the surface profile [19]. We, therefore, present the normalized friction coefficient  $\mu/\nabla z$  instead of  $\mu$  in this Letter.

A typical dependence of the coefficient of friction on the sliding velocity is shown in Fig. 2. At first, it increases linearly with velocity (region I), it then achieves a plateau (region III) and decreases again to a new constant value (region IV). We also marked an intermediate region (II) where transition from the linear velocity dependence to the plateau takes place. This region covers one decade of velocities, and the coefficient of friction increases here by a factor of two. Fig. 3 shows the velocity dependence in double logarithmic scale for 6 different Hurst exponents. It is obvious that at small velocities, the coefficient of friction increases linearly with velocity. The absence of the decreasing region IV in Fig. 3 (and Fig 4 at high loads) is only due to the fact that for high forces this region is outside the scope of practical velocities and is therefore not shown in these figures.

Fig. 4 presents velocity dependencies of the coefficient of friction for 20 different normal forces. One can see that the form of the dependence for different forces is approximately the same, only shifted along the axis of the logarithm of velocity. There are two distinctly different regions: in zone 1 there is a partial contact of the rigid surface and the elastomer, while in zone 2 they are in

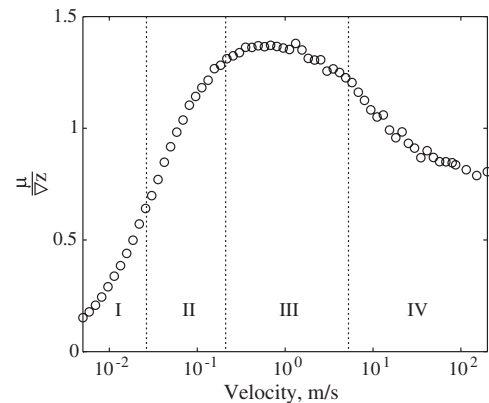


FIG. 2. A typical dependence of the normalized coefficient of friction on the velocity. In this particular case, the results were obtained for the following set of parameters:  $F_N = 0.0034$  N,  $G = 10^7$  Pa,  $h = 5 \times 10^{-7}$  m, and  $H = 0.7$ .

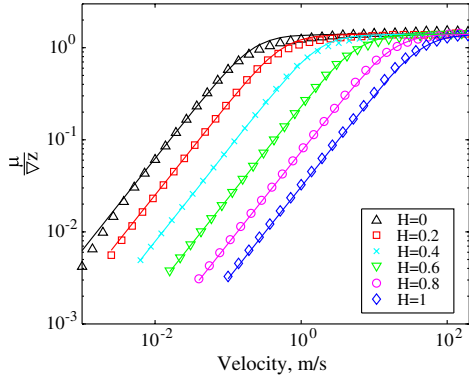


FIG. 3 (color online). Dependence of friction coefficient on velocity for different Hurst exponents and  $F = 10\text{N}$ ,  $G = 10^7\text{ Pa}$ ,  $h = 5 \times 10^{-7}\text{ m}$ . Solid lines correspond to the analytical approximation (11).

complete contact. In both of the zones, the shift factor increases linearly with the logarithm of force, the coefficient of friction, thus, being a power function of the normal force. Simulations with different rms gradients of the surface (which were varied by changing the spacing  $\Delta x$ ) show that the coefficient of friction in this region is very accurately proportional to  $\nabla z^2$  and depends on the force and shear modulus only over the ratio  $F_N/G$ . The only form of the dependence which fits these empirical observations and meets the dimensional demands is

$$\mu = \beta \frac{\tau v \nabla z^2}{h} \left( \frac{G h L}{F_N} \right)^\alpha, \quad (5)$$

where  $\alpha$  and  $\beta$  are dimensionless constants. Empirical values of these constants extracted from numerical data are shown in Fig. 5.

Let us support this result with an analytical estimation. At low velocities, the values of  $z$  in the border points of each partial contact region in the Eq. (4) are the same ( $z = d$ ); thus, the integral  $\int_{\text{real cont}} z'(x) [G(d - z(x))] dx$  vanishes identically. For the coefficient of friction we get

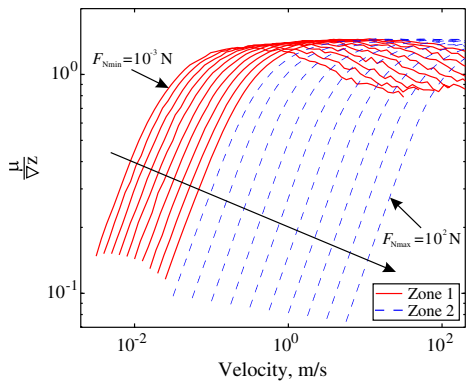


FIG. 4 (color online). Double logarithmic presentation of the dependence of the normalized friction coefficient on velocity for 20 exponentially increasing normal forces ranging from  $10^{-3}$  to  $10^2\text{ N}$ , as indicated by the arrow ( $G = 10^7\text{ Pa}$ ,  $h = 5 \times 10^{-7}\text{ m}$ , and  $H = 0.7$ ). The third line from the left corresponds to the data shown in Fig. 2.

$$\mu = \frac{4L_{\text{cont}} \eta \nabla z_{\text{cont}}^2}{F_N} v. \quad (6)$$

Here,  $L_{\text{cont}}$  is the total contact length and  $\nabla z_{\text{cont}}$  the rms slope in the region of real contact. The rms slope is dominated by the short wavelength part of the spectrum. It can be approximately replaced by the average rms slope of the entire surface  $\nabla z_{\text{cont}} \approx \nabla z$ . At the end of the Letter, we discuss the weak dependence of  $\nabla z_{\text{cont}}$  on loading parameters in more detail.

For small forces, in zone 1, the contact length is a power function of the normal force [17]:  $L_{\text{cont}} \propto F^{1/(1+H)}$ , and the coefficient of friction will be given by  $\mu \propto F^{-H/(1+H)}$ . Comparing this with Eq. (5) provides an analytical estimation for the exponent  $\alpha$ :

$$\alpha = \frac{H}{1+H}. \quad (7)$$

For large normal forces, in zone 2, the contact length achieves a saturation value of  $L_{\text{cont}} = L$ . The coefficient of friction becomes

$$\mu = \frac{4L \eta \nabla z^2}{F_N} v, \quad (8)$$

which is exactly confirmed by numerical simulations. Finally, in the plateau region, the coefficient of friction shows only a weak dependence on the Hurst exponent (Fig. 6). In the range of  $0.2 < H < 0.8$  and for not too small forces, it is almost constant and can be approximated as

$$\mu \approx \sqrt{2} \nabla z_{\text{cont}}. \quad (9)$$

This result has a simple physical meaning. In the plateau region, the elastomer behaves practically as a viscous fluid: the elasticity does not play any role and all contacts are “one-sided.” The normal and tangential forces reduce to  $F_x = 4 \int_{(\text{real cont})} \eta v [z'(x)]^2 dx$ ,  $F_N = 4 \int_{(\text{real cont})} \eta v |z'(x)| dx$ . For the normalized coefficient of friction we get

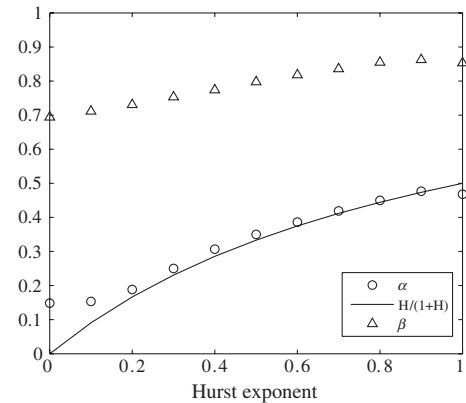


FIG. 5. Dependence of  $\alpha$  and  $\beta$  [see Eq. (5) on the Hurst exponent in zone 1 (see Fig. 4)]. Analytical estimation of the exponent  $\alpha$  according to (7) is shown with the bold line. For  $0.2 < H < 0.8$ , it fits the numerical data very well.

$$\begin{aligned}\mu &= \frac{\int_{(\text{real cont})} (z'(x))^2 dx}{\int_{(\text{real cont})} |z'(x)| dx} \\ &= \nabla z_{\text{cont}} \frac{\left( \int_{(\text{real cont})} (z'(x))^2 dx \right)^{1/2}}{\int_{(\text{real cont})} |z'(x)| dx}.\end{aligned}\quad (10)$$

For an exponential probability distribution function of the gradient of the surface, the ratio of the integrals in (10) is equal to  $\sqrt{2}$ , in accordance with (9), and it depends only weakly on the form of the distribution function.

The results (5) and (7)–(9) can be combined in the following equation providing an interpolation between the three regions I, II, and III:

$$\begin{aligned}\mu &= \left[ \frac{1}{2\nabla z_{\text{cont}}^2} + \left( \frac{F_N}{4L\eta\nabla z_{\text{cont}}^2 v} \right)^2 \right. \\ &\quad \left. + \left( \frac{h}{\beta\tau\nabla z_{\text{cont}}^2 v} \left( \frac{F_N}{GhL} \right)^{\frac{H}{1+H}} \right)^2 \right]^{-1/2}.\end{aligned}\quad (11)$$

The quality of this interpolation can be seen in Fig. 3 where the numerical results for six Hurst exponents are plotted together with analytical dependencies (11). This equation can be rewritten in the dimensionless form

$$\bar{\mu} = \left[ 1 + \frac{((\bar{F}_N/4)^2 + (\bar{F}_N)^{\frac{2H}{1+H}})}{\bar{v}^2} \right]^{-1/2}, \quad (12)$$

with a normalized coefficient of friction  $\bar{\mu} = \mu / (\sqrt{2}\nabla z_{\text{cont}})$ , dimensionless velocity

$$\bar{v} = \frac{\tau v \nabla z_{\text{cont}}}{\sqrt{2}h}, \quad (13)$$

and dimensionless force

$$\bar{F}_N = \frac{F_N}{GhL}. \quad (14)$$

Let us discuss the physical meaning of the quantities  $\bar{v}$  and  $\bar{F}_N$ . The condition  $\bar{F}_N \approx 1$  gives the order of magnitude of the force at which complete contact is achieved, while the condition  $\bar{v} \approx 1$  determines the order of magnitude of

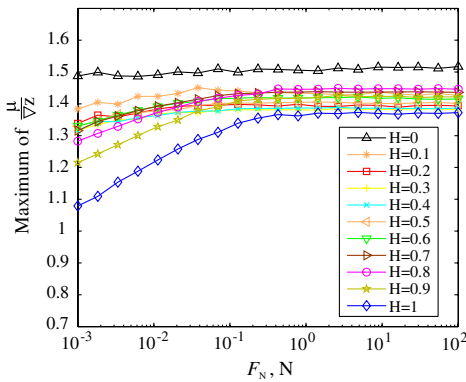


FIG. 6 (color online). Dependence of the normalized coefficient of friction in region III (plateau). The coefficient of friction decreases at very small forces. This effect is closely related to the decrease of the coefficient of friction at high sliding velocities, Fig. 2, in region IV.

velocity at which the elastomer is detached from the rigid surface on the trailing side of any asperity and all the contacts become “one-sided.” Indeed, according to (2), the condition of detachment  $f = 0$  means  $d - z(x) + \eta v z'(x) = 0$ . Taking into account that  $d - z$  has the order of magnitude of  $h$  and  $z'$  has the order of magnitude of  $\nabla z_{\text{cont}}$ , we come to the conclusion that the one-sided detachment of the elastomer will occur if  $(\eta/G)v\nabla z_{\text{cont}} > h$  or  $\bar{v} > 1$ . Note that the same conditions are valid in the corresponding three-dimensional problem: for achieving the plateau value of contact stiffness ( $\bar{F}_N \approx 1$ , [17]) and for the one-sided detachment of the elastomer ( $\bar{v} \approx 1$ ).

Let us discuss the decrease of the coefficient of friction beyond the region of validity of approximation (12), at large velocities (region IV in Fig. 2). Such a decrease at large velocities is typical for elastomer friction and is usually associated with a decrease in the “rheological factor”  $\text{Im}G(\omega)/|G(\omega)|$  at high frequencies [6], where  $G(\omega)$  is the complex modulus of the elastomer and  $\text{Im}G(\omega)$  its imaginary part. For the case of the Kelvin body, however, the rheological factor is equal to  $\eta\omega/\sqrt{G^2 + (\eta\omega)^2}$ ; it increases monotonically and tends towards 1 at high frequencies. In this case, the decrease of the coefficient of friction is not related to the rheology but rather to the dependence of the rms slope on the size of the real contact. Indeed, for randomly rough surfaces, the rms slope in the contact region can be estimated as

$$\begin{aligned}\nabla z_{\text{cont}} &= \left( 2 \int_{q_{\text{cont}}}^{q_{\text{max}}} C_{\text{ID}}(q) q^2 dq \right)^{1/2} \\ &\propto \left( \frac{[q_{\text{max}}^{-2(1-H)} - q_{\text{cont}}^{-2(1-H)}]}{2(1-H)} \right)^{1/2},\end{aligned}\quad (15)$$

where the lower integration limit  $q_{\text{cont}} \approx 2\pi/L_{\text{cont}}$  decreases with increasing size of the real contact. For  $0 < H < 1$ , the integral (15) depends only weakly on the lower integration limit unless the contact length becomes extremely small so that  $q_{\text{cont}}$  approaches  $q_{\text{max}}$ . Thus, the coefficient of friction in the region of plateau will decrease with decreasing indentation depth. This happens either at extremely high sliding velocities (Fig. 2, region IV) or at extremely low normal forces as illustrated in Fig. 6. The dependence of  $\nabla z_{\text{cont}}$  on the contact size and, thus, on velocity and force is less pronounced for small Hurst exponents,  $H \approx 0$ , and gets stronger for  $H \approx 1$ . Note that the increase of rms slope with increasing indentation is closely associated with the assumption of the “randomness” of roughness, as the estimation (15) is only valid if the Fourier components of roughness with different wave vectors have uncorrelated phases. One can say that randomly rough surfaces are always rougher on the slopes of waviness than on the summits. Real surfaces, on the contrary, may have different kinds of correlated roughness. One can easily imagine a surface, which is rougher on the summits than on the slopes; for such surfaces, the rms slope of roughness would decrease with indentation. The general and robust statement, which is independent of the kind of the roughness correlation, is only that the rms slope in the contact

region is a function of indentation depth and, thus, a function of the nondimensional force (14). This statement even remains valid if the linear viscoelastic behavior of the material breaks down at the microscale. Indeed, the statement that the frictional force will depend on the indentation depth is correct for any kind of processes at the microscale. The indentation depth, however, is governed by the contact stiffness which is dominated by the largest wavelength in the power spectrum of the roughness. The general conclusions that the nondimensional force (14) is a governing parameter of the friction process will, therefore, remain valid independently of the particular character of the microscopic processes. We can summarize our results to the following general scaling relation:

$$\mu = \nabla_{z_{\text{cont}}}(\bar{F}_N)g[\bar{v}/f(\bar{F}_N)], \quad (16)$$

or, in explicit form,

$$\mu = \nabla_{z_{\text{cont}}}\left(\frac{F_N}{GhL}\right)g\left[\frac{\tau v \nabla_{z_{\text{cont}}}}{\sqrt{2}h} / f\left(\frac{F_N}{GhL}\right)\right]. \quad (17)$$

This scaling relation means that the dependence of the coefficient of friction on velocity in the *double logarithmic* presentation has the same form for different values of all parameters appearing in this equation: force  $F_N$ , size of the system  $L$ , and relaxation time  $\tau$ . Changing of any of these parameters will only shift the curves horizontally by the factor of  $\approx \log[\frac{\tau \nabla_{z_{\text{cont}}}}{\sqrt{2}h} / f(\frac{F_N}{GhL})]$  and vertically by the factor of  $\log \nabla_{z_{\text{cont}}}(F_N/GhL)$ . In particular, the curves will be shifted by changes of temperature (which influences the relaxation time). The shifting procedure with regard to temperature is well known and widely used in the physics of friction of elastomers for constructing “master curves” describing the friction coefficient at any velocity and temperature (see, e.g., [22]). Eq. (17) means that the master curve procedure can be generalized to dependencies on other loading and system parameters. While the particular form (11) of the law of friction is limited by the assumptions of simple viscoelastic rheology, the general scaling relation (17) should have a wider range of application and it should be possible to validate it experimentally.

In conclusion, we have shown that the law of friction between a linear viscoelastic body and a rigid fractal surface can be formulated in terms of two dimensionless variables (13) and (14) which are proportional to the sliding velocity and the normal force, correspondingly. Over these variables, the force of friction generally depends on all material, loading, and roughness parameters: sliding velocity, normal force, shear modulus, viscosity, rms roughness, rms slope, and even the size of the system. Generally, the force of friction is not proportional to the normal force; thus, Amonton’s law is violated. However, in the plateau region, where the coefficient of friction achieves its maximum, it is proportional to the rms slope of the roughness in the contact region and depends only weakly on the normal force or any other system parameter. We provided physical interpretation of the dimensionless variables and a simple

interpolation equation summarizing all numerical and analytical data for a surface with self-affine roughness having Hurst exponents in the range from 0 to 1. One of the implications of the obtained analytical results is the generalization of the master curve procedure to further variables such as the normal force and the size of the system. We argued that the main physics of the frictional process are dimension invariant. In particular, the general scaling relations should retain their validity for three-dimensional systems.

We would like to thank R. Pohrt and J. Benad for valuable discussions. This work was supported by the Deutsche Forschungsgemeinschaft (DFG), the German Academic Exchange Service (DAAD), and the Federal Ministry of Economics and Technology (Germany) under the Contract No. 03EFT9BE55, Q. Li was supported by a scholarship from the China Scholarship Council (CSC).

\*Corresponding author.

v. popov@tu-berlin.de

- [1] F. P. Bowden and D. Tabor, *The Friction and Lubrication of Solids* (Clarendon Press, Oxford, 1986).
- [2] J. A. Greenwood and D. Tabor, *Proc. R. Soc. A* **71**, 989 (1958).
- [3] K. A. Grosch, *Proc. R. Soc. A* **274**, 21 (1963).
- [4] M. Barquins and R. Courtel, *Wear* **32**, 133 (1975).
- [5] M. Klüppel and G. Heinrich, *Rubber Chem. Technol.* **73**, 578 (2000).
- [6] B. N. J. Persson, *J. Chem. Phys.* **115**, 3840 (2001).
- [7] B. Lorenz, B. N. J. Persson, G. Fortunato, M. Giustiniano, and F. Baldoni, *J. Phys. Condens. Matter*, **25**, 095007 (2013).
- [8] V. L. Popov and A. Dimaki, *Tech. Phys. Lett.* **37**, 8 (2011).
- [9] A. Schallamach, *Proc. R. Soc. Edinburgh, Sect. B Biol.* **65**, 657 (1952).
- [10] O. Ben-David and J. Fineberg, *Phys. Rev. Lett.* **106**, 254301 (2011).
- [11] M. Otsuki and H. Matsukawa, *Sci. Rep.* **3**, 1586 (2013).
- [12] S. M. Rubinstein, G. Cohen, and J. Fineberg, *Nature (London)* **430**, 1005 (2004).
- [13] O. Ben-David, G. Cohen, and J. Fineberg, *Science* **330**, 211 (2010).
- [14] D. S. Amundsen, J. Scheibert, K. Thøgersen, J. Trømborg, and A. Malthe-Sørenssen, *Tribol. Lett.* **45**, 357 (2012).
- [15] M. Heß, *About Mapping of Some Three-Dimensional Contact Problems to Systems with a Lower Spatial Dimensionality* (Cuvillier-Verlag, Göttingen, 2011).
- [16] M. Heß, *Phys. Mesomech.* **15**, 264 (2012).
- [17] R. Pohrt, V. L. Popov, and A. E. Filippov, *Phys. Rev. E* **86**, 026710 (2012).
- [18] S. Kürschner and V. L. Popov, *Phys. Rev. E* **87**, 042802 (2013).
- [19] V. L. Popov, *Contact Mechanics and Friction. Physical Principles and Applications* (Springer-Verlag, Berlin, 2010), p. 362.
- [20] V. L. Popov and M. Heß, *Method of Dimensionality Reduction in Contact and Friction: A Calculation Methodology for Micro- and Macro Systems* (Springer, Berlin, 2013).
- [21] V. L. Popov, *Friction and wear in machinery* **1**, 41 (2013).
- [22] A. Le Gal, X. Yang, and M. Klüppel, *J. Chem. Phys.* **123**, 014704 (2005).